© 2018. Published by The Company of Biologists Ltd | Journal of Cell Science (2018) 131, jcs209155. doi:10.1242/jcs.209155

RESEARCH ARTICLE

APC/C^{Fzr} regulates cardiac and myoblast cell numbers, and plays a crucial role during myoblast fusion

Maik Drechsler*,‡, Heiko Meyer, Ariane C. Wilmes and Achim Paululat‡

ABSTRACT

Somatic muscles are formed by the iterative fusion of myoblasts into muscle fibres. This process is driven by the recurrent recruitment of proteins to the cell membrane to induce F-actin nucleation at the fusion site. Although several proteins involved in myoblast fusion have been identified, knowledge about their subcellular regulation is rather elusive. We identified the anaphase-promoting complex (APC/C) adaptor Fizzy related (Fzr) as an essential regulator of heart and muscle development. We show that APC/C^{Fzr} regulates the fusion of myoblasts as well as the mitotic exit of pericardial cells, cardioblasts and myoblasts. Surprisingly, overproliferation is not causative for the observed fusion defects. Instead, *fzr* mutants exhibit smaller F-actin foci at the fusion site and display reduced membrane breakdown between adjacent myoblasts. We show that lack of APC/C^{Fzr} causes accumulation and mislocalisation of Rols and Duf, two proteins involved in the fusion process. Duf seems to serve as direct substrate of the APC/C^{Fzr} and its destruction depends on the presence of distinct degron sequences. These novel findings indicate that protein destruction and turnover constitute major events during myoblast fusion.

KEY WORDS: Myoblast fusion, Muscle, *Fizzy related*, APC/C, Cdh1, Dumbfounded, Rolling pebbles, Cell cycle, *Drosophila*

INTRODUCTION

Fizzy related (Fzr) constitutes an adaptor protein of the large E3 ubiquitin ligase anaphase-promoting complex/cyclosome (APC/C), a key player of the ubiquitin-proteasome degradation pathway. Fzr serves as a co-activator of the APC/C, essential for recognition and recruitment of substrate proteins to the complex for polyubiquitylation, a post-translational modification that usually causes destruction of the marked protein by the proteasome (Chang and Barford, 2014). Classic targets of the complex include securins, which regulate metaphase-anaphase transition (Acquaviva and Pines, 2006; Follette and O'Farrell, 1997) and cyclins, main regulators of cell cycle progression (Han et al., 2009; Solomon and Burton, 2008). Moreover, APC/C^{Fzr} regulates the transition from mitosis into endoreplication cycles in the *Drosophila* salivary gland, leading to the formation of polytene chromosomes (Zielke et al., 2008). Besides its well-known function during mitosis, the APC/C has been shown to also have essential cell-cycle-independent roles (for example, see Braun et al., 2018 preprint; Martins et al., 2017; Meghini et al., 2016; Neuert et al., 2017; Silies and Klämbt, 2010; van Roessel et al., 2004; Weber and Mlodzik, 2017).

Here we describe a dual role of the APC/C^{Fzr} during embryonic heart and muscle development in *Drosophila*. We show that the APC/C^{Fzr} is crucial to regulate the number of pericardial cells (PCs), cardioblasts (CBs) and myoblasts. More importantly, we found that it also controls the fusion of myoblasts into mature muscle fibres. Typically, somatic muscles are syncytial and differentiate by cell–cell fusion. In the *Drosophila* embryo, myogenesis constitutes a multi-step process, including the determination of specific myoblast subtypes, cell cycle exit and heterogenic fusion of myoblasts. Fusion occurs between two distinct sets of myoblasts – founder cells (FCs) and fusion-competent myoblasts (FCMs). The former act as a 'seed' for a specific muscle and their genetic programme encodes a specific muscle identity; this identity determines the size, location and attachment points of each individual muscle cell. The latter act as fusion mass, allowing the FCs to grow into larger, syncytial muscle fibres by iterative rounds of fusion. After their determination, one FC initially fuses with one to two FCMs to form a muscle precursor. In a second round, and in parallel to myotube guidance and attachment, a defined number of additional FCMs fuses with the precursor one after another. Eventually, the myotubes stabilize their attachment to the epidermis and the formation of sarcomeres concludes (for reviews, see Rochlin et al., 2010; Schulman et al., 2015).

In our present study, we analysed a set of *fzr* mutant alleles, which exhibit an arrest of myoblast fusion after initial muscle precursor formation. Excess myoblasts adhere to the precursors and characteristic F-actin foci form on the presumptive fusion site. However, those F-actin foci are smaller than in wild type, fusion pore formation and membrane breakdown at the fusion site is inhibited and, subsequently, fusion is blocked. We provide the first evidence that the APC/C^{Fzr} is essential for myogenesis *in vivo*, and acts during the second phase of fusion during myogenesis in *Drosophila*.

RESULTS

Loss of *fzr* causes myoblast fusion defects

To identify new regulators of heart and muscle development, we screened a collection of ethyl methanesulfonate (EMS)-induced mutations, located on the X chromosome, that exhibit embryonic lethality (Hummel et al., 1999). By staining for the muscle-specific protein β3 tubulin (β3Tub) we identified three EMS-induced alleles of *fzr* that showed aberrant muscle and heart morphologies (Fig. 1A-H and Fig. 3). While previously a deficiency that contains the *fzr* gene locus has been shown to cause muscle defects, *fzr* itself has not been linked to myogenesis so far (Drysdale et al., 1993).

Hemizygous fzr^{G129}, fzr^{H089} or fzr^{J053} mutants displayed an arrest of myoblast fusion, indicated by the appearance of small 'mini

University of Osnabrück, Department of Zoology and Developmental Biology, Barbarastraße 11, 49076 Osnabrück, Germany.
*Present address: University of Cambridge, Department of Zoology, CB2 3EJ, Cambridge, UK.

‡Authors for correspondence (drechsler@biologie.uni-osnabrueck.de; paululat@biologie.uni-osnabrueck.de)

M.D., 0000-0001-7484-6365

Received 2 August 2017; Accepted 30 May 2018

Journal of Cell Science (2018) 131, jcs209155. doi:10.1242/jcs.209155

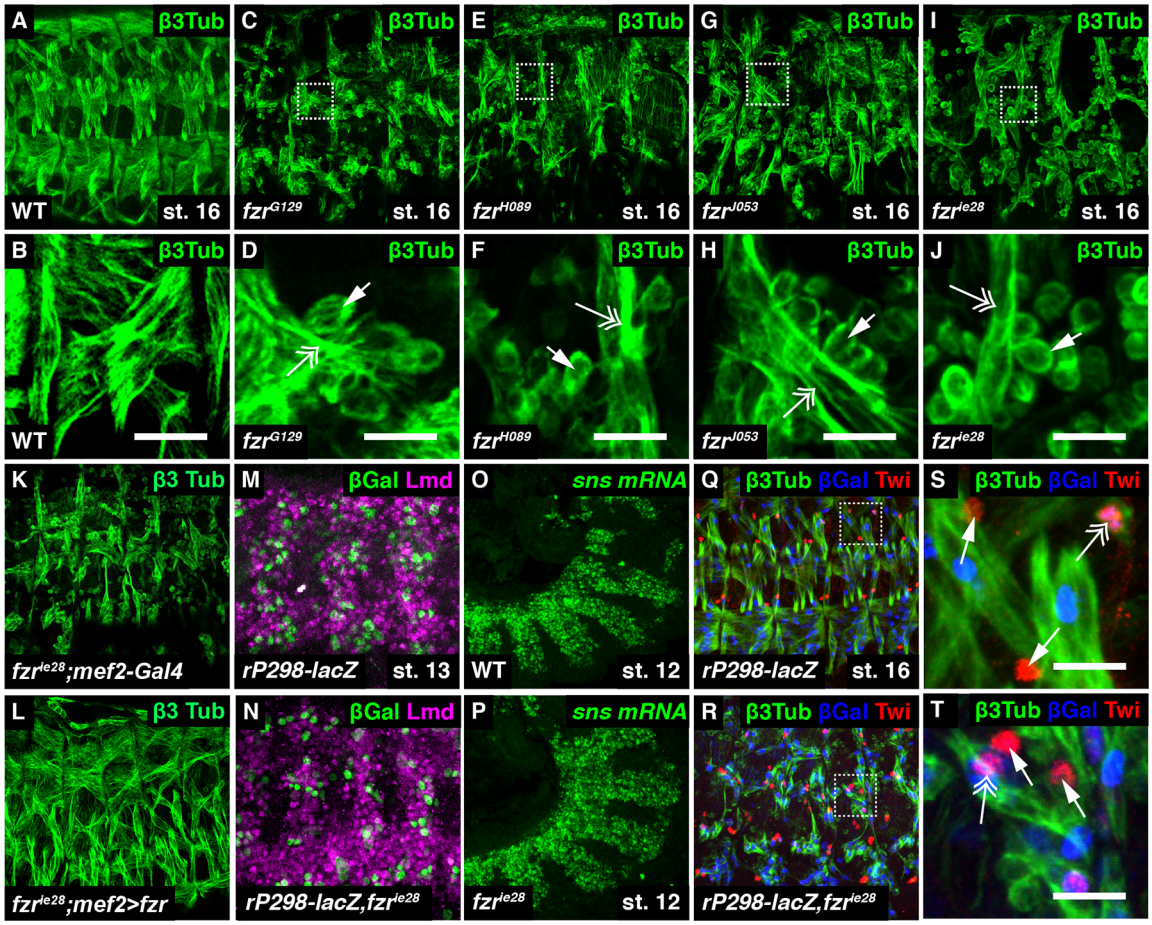

Fig. 1. Mutations in *fzr* cause myoblast fusion defects. (A-J) Stage 16 embryos stained with anti-β3Tub antiserum. Mutant embryos (four to five hemisegments) exhibit strong myoblast fusion defects. The musculature of mutants only comprises small muscle fibres (double-headed arrows). Additionally, a variable number of unfused myoblasts is seen, some attaching to the small myotubes, indicating an arrest in cell-cell fusion (arrows). Boxed areas indicate magnified image below. (K,L) Re-expression of *fzr* in all myoblasts of the amorphic allele fzr^{ie28} partially restores fusion. (M,N) Stage 13 embryos stained with anti-βGal (FC) and anti-Lmd (FCM) antibodies. Staining indicates that both cell populations are present in mutant embryos. (O,P) Transcripts of *sns* (FCM) at stage 12 can be detected in wild type and mutant embryos at about the same expression levels. (Q-T) Stage 16 embryos stained with anti-β3Tub, anti-βGal and anti-Twist antibodies, to visualize outline (β3Tub) and nuclei (βGal) of all muscles and adult muscle precursors (AMPs), respectively. Twist-positive AMPs are indicated by arrows. Additionally, lacZ- and Twi-positive alary cells (Bate et al., 1991), are present in wild type and mutant animals (double-headed arrows); boxed areas indicate magnified images to the right. Scale bars: 10 µm.

muscles' and an excess of mono-nucleated myoblasts (Fig. 1A-H). Some of those solitary myoblasts were still attached to the small muscles, suggesting that myoblast migration, recognition and adhesion took place in mutant embryos (Fig. 1B,D,F,H). The alleles fzr^{G129} and fzr^{H089} have been characterised before, and both exhibit premature stop codons resulting in truncated protein versions (Silies and Klämbt, 2010). Although some variability was observed, it seems that hemizygous fzr^{J053} mutants exhibited more unfused myoblasts and, probably, larger remaining muscles, suggesting it to be the weakest of the three EMS alleles (compare Fig. 1H to D,F). Nevertheless, fzr^{J053} failed to complement fzr^{ie28}, a known protein null mutant (Jacobs et al., 2002) that showed similar fusion defects (Fig. 1I,J; Materials and Methods; data not shown). Since not all of the new *fzr* alleles have been sequenced, and since it is unclear whether the truncated proteins expressed in fzr^{G129} and fzr^{H089} cause any dominant effects, we decided to use the amorphic allele fzr^{ie28} for most of the following experiments.

fzr encodes an adaptor protein of the APC/C, a large E3-ubiquitin ligase that is conserved amongst all eukaryotes, and best characterised for its role during cell cycle progression (Han et al., 2009; Solomon and Burton, 2008). Although the mammalian homologue of *fzr* (*Cdh1*) has been implicated in regulating cell cycle withdrawal, differentiation and probably fusion of cultured myoblasts, the function of the APC/C^{Fzr} during myogenesis has never been addressed *in vivo* (Li et al., 2007). In *Drosophila*, the lack of *fzr* causes cell division and cell migration defects in the epidermis and the nervous system (Jacobs et al., 2002; Sigrist and Lehner, 1997; Silies and Klämbt, 2010), and Fzr is involved in size regulation of synapses (van Roessel et al., 2004). To exclude that the observed myoblast fusion phenotype is due to a function in any non-muscular tissue, we re-expressed *fzr* in mutant myoblasts. This resulted in a rescue of the myoblast fusion phenotype, strongly arguing for a cell-autonomous function of *fzr* during myogenesis (Fig. 1K,L).

The somatic musculature in the *Drosophila* embryo is formed by two distinct cell populations – FCs and FCMs. In the early embryo, FC progenitors are singled out from groups of equally competent cells by lateral inhibition, while the remaining cells become determined as FCMs. The progenitors further divide asymmetrically, to give rise to either two FCs, one FC and one adult muscle precursor (AMP), two AMPs, or one FC and a set of PCs (reviewed by Dobi et al., 2015). To asses, whether all of these cell populations were determined in *fzr* mutants, we monitored the expression of cell-specific molecular

Journal of Cell Science (2018) 131, jcs209155. doi:10.1242/jcs.209155

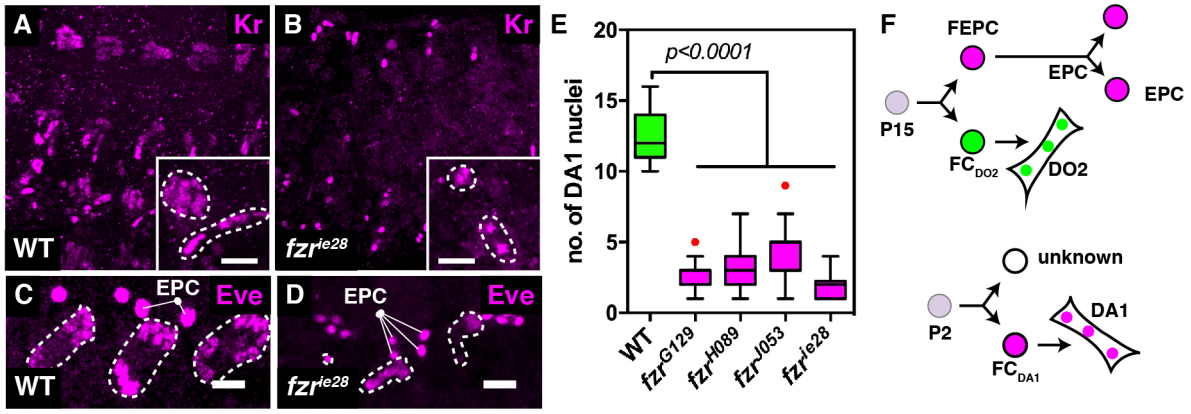

Fig. 2. Fusion arrests after precursor formation in *fzr* mutants. (A-D) Stage 15 embryos stained with anti-Kr antibodies (five hemisegments) or anti-Eve antibodies (three hemisegments) to reveal different FC populations as well as EPCs (pointers in C,D). Most Kr- or Eve-positive muscles in *fzr* mutants exhibited only 1–3 nuclei, indicating an arrest of fusion after precursor formation (encircled areas in A, B (insets) and C, D). In contrast, the number of EPCs was increased (pointers in C and D). (E) Numbers of Eve-positive DA1 nuclei are severely reduced in different *fzr* mutant alleles. (F) Lineages of EPCs and DA1 FCs (re-drawn according to Han and Bodmer, 2003). EPCs and DA1 founder cells segregate from two different mesodermal progenitor cells (P15 and P2, respectively). Asymmetric division of P2 gives rise to the DA1 founder (FC_{DA1}) and a cell of unknown fate. Asymmetric division of P15 gives rise to the founder cell of muscle DO2 (FC_{DO2}) as well as a founder cell of the EPCs (FEPC), that in turn divides one more time in a symmetric manner to give rise to two EPCs per hemisegment. Scale bars: 10 µm.

markers (Fig. 1M-T). First, we visualised expression of the FC-specific reporter gene rP298-lacZ (Nose et al., 1998) and the FCM-specific transcription factor Lame duck (Lmd) (Duan et al., 2001; Ruiz-Gómez et al., 2002). Upon fusion, the nuclei of the nascent muscles started to express the *lacZ* reporter gene, while at the same time they stopped expressing Lmd. At late stage 13, just after the onset of fusion, nuclei showing expression of either protein were found in wild type and *fzr* mutant embryos, suggesting that FCs and FCMs become specified, and that the segregation of the main myogenic cell lineages takes place (Fig. 1M,N). Furthermore, the FCM-specific gene *sns* (Bour et al., 2000; Haralalka and Abmayr, 2010) was expressed in wild type and mutant embryos at comparable transcript levels, indicating that FCMs do not just segregate but also differentiate correctly (Fig. 1O,P and Fig. 7A-C). To test for the presence of AMPs, we stained for Twist (Twi), a transcription factor expressed in the early mesoderm that remains expressed in all AMPs (Bate et al., 1991). In each hemisegment of the embryo, six AMPs are found at distinct positions along the dorsal-ventral axis (Fig. 1Q and Figeac et al., 2010). In addition, each hemisegment contains a set of Twi-positive cells, the so-called alary cells, that also show expression of the rP298-lacZ reporter gene (see Bate et al., 1991; and double headed arrows in Fig. 1S,T). Both cell populations were present in *fzr* mutants, further indicating that all cell lineages of the myogenic mesoderm segregate (Fig. 1Q-T).

In summary, our initial experiments strongly suggest that the determination of myoblasts as well as their differentiation into FCM and FC populations take place in mutant embryos, and that *fzr* presumably plays a role during myoblast fusion.

Myoblast fusion arrests after precursor formation in *fzr* mutants

Syncytial muscles in the *Drosophila* embryo are formed by the iterative fusion of a single FC with a specific number of FCMs, initially leading to the formation of a bi- or tri-nucleated muscle precursor. In a second round of fusion, the precursor recruits more FCMs, allowing the muscle to grow in size until fusion terminates (Bate, 1990). Identity, size and attachment sites of each individual muscle are determined by the FC-specific expression of identity transcription factors, including Kr and Eve (Bataillé et al., 2010; Knirr et al., 1997; Ruiz-Gómez et al., 1997; Su et al., 1999). Upon fusion, they become expressed by all nuclei within each syncytium, thus, their expression can be used to monitor the number of cells fused into one muscle (Fig. 2). Staining for Kr in stage 15 embryos revealed that the number of Kr-positive nuclei per muscle was severely reduced in *fzr* mutants (insets in Fig. 2A,B). Nevertheless, Kr-expressing muscles with two, or sometimes three nuclei could be found, suggesting that the first round of fusion and, therefore, precursor formation takes place. To directly assess the exact time point at which fusion was stalled in mutant embryos, we counted the number of the Even skipped (Eve)-positive nuclei in DA1 muscle cells (Fig. 2C-E). On average, the number of Eve-expressing nuclei in muscle DA1 was reduced by a factor of four in all *fzr* alleles (Fig. 2E and Table S1). However, we frequently found muscles with two or more nuclei. This suggests that, similarly to Kr-positive muscles, DA1 cells are able to undergo the initial round of fusion and form muscle precursors, and that fusion stalls during the second fusion wave. Eve is also expressed in a subset of PCs – the Eve-positive pericardial cells (EPCs) – that are loosely attached to the heart of the embryo. These are located dorsally of muscle DA1 and are easily distinguished from the muscle cells because they show stronger expression of Eve and do not express the reporter rP298-lacZ (Fig. 2C and data not shown). In contrast to the number of nuclei in muscle DA1, the number of EPCs is markedly increased in *fzr* mutants (Fig. 2C,D and Table S1). Although they do express Eve, EPCs are no direct siblings of the DA1 FCs. Instead, they are formed by symmetric division of a founder of EPC (FEPC) progenitor cell that, in turn, is a sibling of the founder of muscle DO2 (FC_{DO2}) (Fig. 2F). Therefore, EPCs naturally undergo one more division compared to FCs (Han and Bodmer, 2003). However, these data indicate that EPCs fail to exit mitosis in *fzr* mutants and undergo at least one more division, leading to a nearly doubled number of cells.

Taken together, our results suggest that the lack of *fzr* causes a block of myoblast fusion after the initial formation of muscle precursors and has a profound effect on the number of a subset of PCs. This observation led us to question whether other heart-associated cell types are also affected by the lack of *fzr*.

Journal of Cell Science (2018) 131, jcs209155. doi:10.1242/jcs.209155

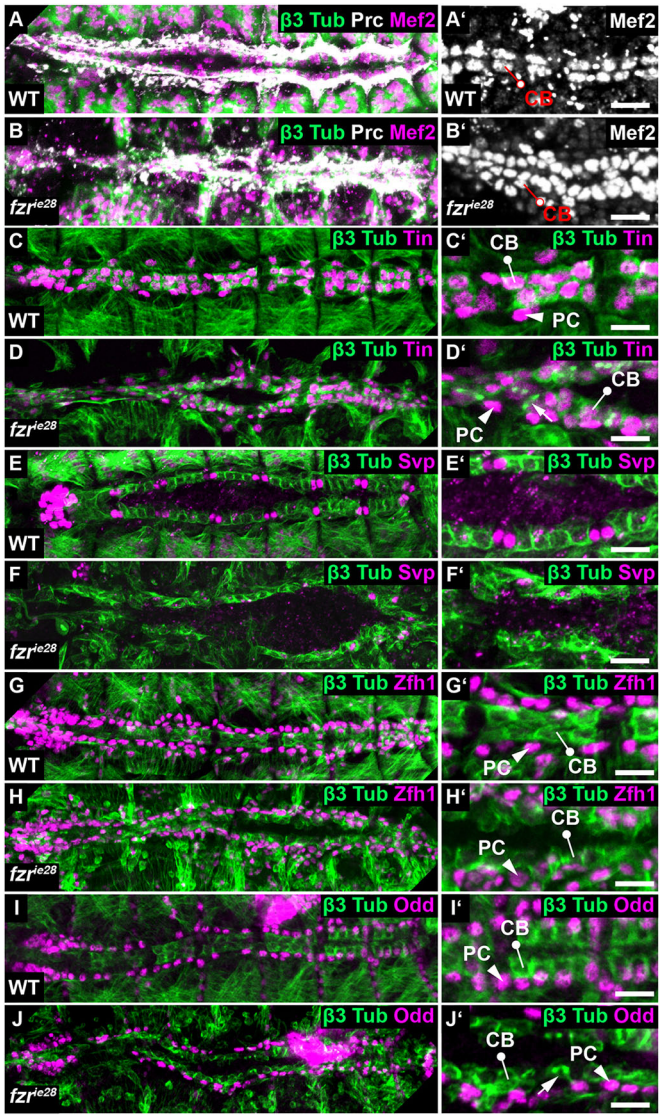

Fig. 3. Altered heart morphology and cell numbers in *fzr* mutants. (A-J) Stage 16 and 17 wild type (WT) and fzr^{ie28} embryos stained for different CB and PC markers; A′-J′ are respective magnified images. Secretion of Prc indicates the correct determination and differentiation of PCs (A,B). CBs showed misalignment and crowding, and the observed elevated CB numbers indicated overproliferation in *fzr* mutants (A′,B′). (C,C′,C,D′) Tin-expressing CBs and PCs are misaligned and increased in number. Tin-positive CBs frequently display abnormal β3Tub accumulation (arrow in D′). (E,E′,F,F′) In contrast, the number of Svp-positive CBs appears strongly reduced. (G,G′,H,H′,I,I′,J,J′) Zfh1-positive and Odd-positive PCs accumulate in clusters along the heart tube and exhibit increased numbers. Arrows indicate abnormal β3Tub accumulations, pointers indicate CBs, arrowheads indicate PCs. Scale bars: 10 µm.

Mutation of *fzr* causes altered cardiac morphology and increased cell numbers

During our initial assessment of mutants, we found that, in addition to aberrant myogenesis, all *fzr* alleles exhibited morphological defects of the cardiac system (Fig. 3). The dorsal vessel (or heart) of the fly constitutes a linear, tubular organ, situated at the dorsal side of the embryo. It is formed by CBs that differentiate into contractile cardiomyocytes by the end of embryogenesis. The heart is attached to a heterogeneous group of PCs via a specialised extracellular matrix (ECM) (Drechsler et al., 2013; Volk et al., 2014; Rotstein et al., 2018; Wilmes et al. 2018). While cardiomyocytes provide the contractile forces to pump hemolymph through the body, the role of PCs is more complex. In the embryo, most PCs secrete ECM proteins to ensure proper establishment of cell-cell contacts. After embryogenesis, only few PCs survive and differentiate into pericardial nephrocytes – scavenger cells allowing an effective filtering of the hemolymph (Ivy et al., 2015, Psathaki et al., 2018).

To assess whether CBs and PCs are determined in *fzr* mutants, we first stained stage 17 embryos for the myogenic transcription factor Mef2, expressed in all CBs (Lilly et al., 1994), and the secreted ECM protein Pericardin (Prc) (Chartier et al., 2002) (Fig. 3A,B). The dense accumulation of Prc in mutant embryos, indicated that PCs do segregate and are able to secrete ECM proteins (Fig. 3B). Staining for Mef2 showed that CBs are determined as well, and do migrate towards the dorsal midline of the embryo. However, while in wild type embryos CBs were strictly aligned in a double row of cells, they appeared misaligned and crowded in *fzr* mutants (Fig. 3A′,B′). Counting all Mef2-positive CBs revealed a slight, but statistically significant increase of cell number (Table S1). To investigate this phenotype in more detail, we visualised specific subgroups of CBs and PCs. β3Tub and Tinman (Tin), an essential transcription factor for heart development, are expressed in eight out of twelve CBs per segment, while Tin is also expressed in various PCs (Azpiazu and Frasch, 1993; Bodmer, 1993; Kremser et al., 1999). In wild type, Tin- and β3Tub-positive CBs were packed in a tight and regular array in each segment, separated by four CBs that express the hormone receptor Seven up (Svp) (Fig. 3C-F) (Gajewski et al., 2000; Lo and Frasch, 2001). Loss of *fzr* abolished this regular pattern, and Tin- and β3Tub-positive CBs as well as Tin-positive PCs accumulated in irregular clusters (Fig. 3D,D′). Strikingly, the expression of Svp was largely abolished from mutant embryos (Fig. 3E,E′,F,F′). However, the elevated numbers of Mef2-positive cells indicated a general increase in CB number (Table S1), and suggest that the loss of Svp-expressing cells is not due to an overall reduction of CBs but, rather, reflects a problem in the differentiation of those cells. Furthermore, since counting Mef2-positive CBs only showed a mild increase, we concluded that the majority of extra Tin-positive cells seem to be PCs. To verify this hypothesis, we used immunostaining against a general marker of all PCs Zfh1 and Odd skipped (Odd), which is expressed in the PC subpopulation that will differentiate into larval nephrocytes (Fig. 3H-J) (Das et al., 2008; Lai et al., 1991; Ward and Skeath, 2000). With some variability, we found larger clusters of Zfh1-expressing cells along the heart tube (Fig. 3G,H). Counting the number of Odd-positive cells revealed a marked increase in mutant embryos, further supporting the observation that loss of *fzr* causes elevated PC numbers (Fig. 3I,J and Table S1). These results suggest that CBs and PCs are not exiting mitosis correctly, and are able to induce extra rounds of cell division, an interpretation that fits the known function of APC/C^{Fzr} in regulating cell cycle exit.

APC/C^{Fzr}-mediated regulation of myoblast number and fusion functions independently of each other

To elucidate whether *fzr* regulates myogenesis in concert with the APC/C we generated double mutants of *fzr* and alleles of two APC/C subunits-APC11/*lemming* (*lmg*) and APC2/*morula* (*mr*) (Nagy et al., 2012; Reed and Orr-Weaver, 1997). Homozygous mutants for either *lmg* (Fig. 4A,A′) or *mr* (Fig. 4B,B′) did not show muscle defects. Transheterozygous *fzr*/+; *lmg*/+ (Fig. 4C) or *fzr*/+; *mr*/+ (Fig. 4D) embryos exhibited an overall normal muscle morphology. However, single unfused myoblasts, attaching to differentiated myotubes, frequently accumulated in *fzr*/+; *lmg*/+ (Fig. 4C′) and, more prominently, in *fzr*/+; *mr*/+ embryos (Fig. 4D′)

Journal of Cell Science (2018) 131, jcs209155. doi:10.1242/jcs.209155

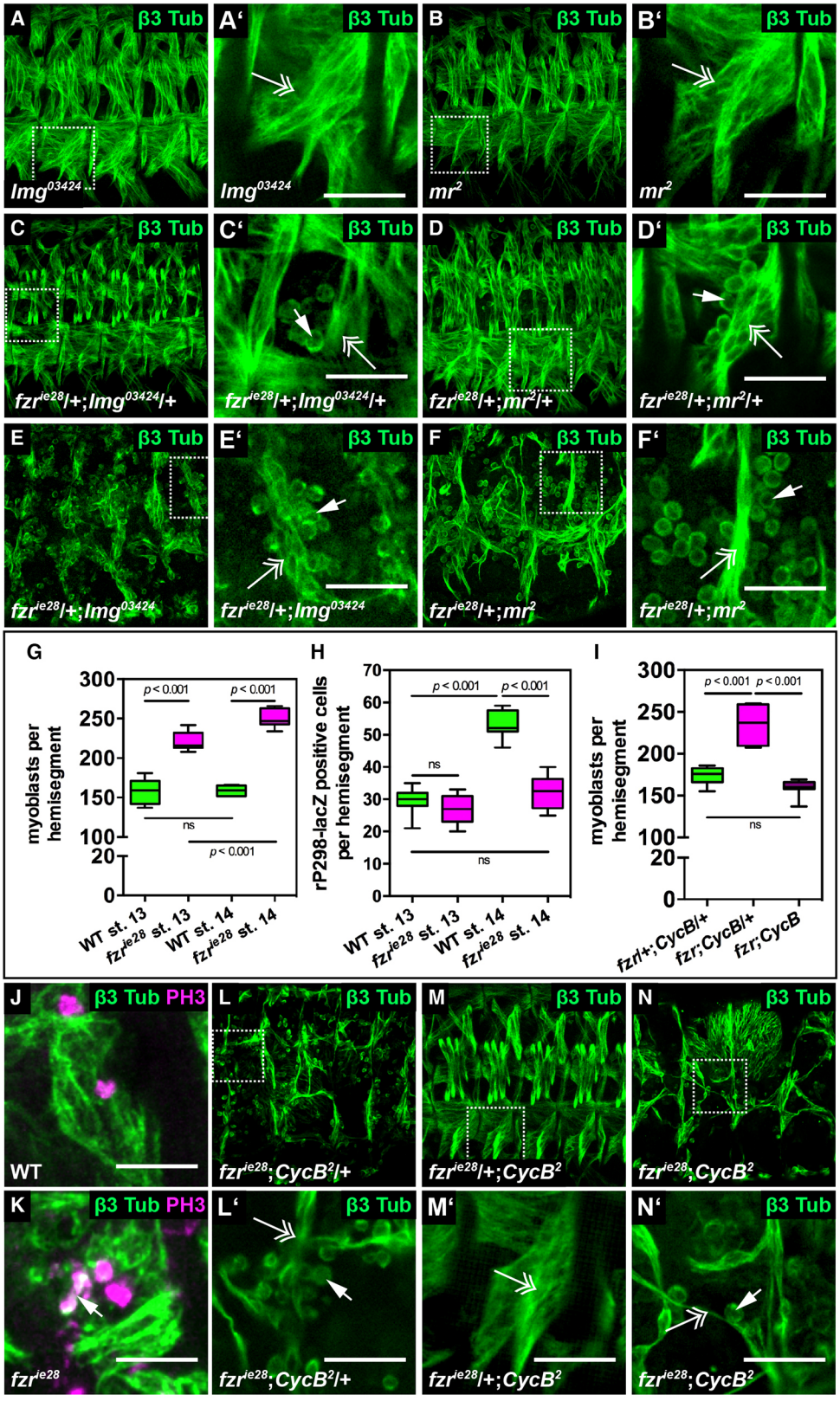

Fig. 4. Dual role of APC/C^{Fzr} during myogenesis. (A-F′) Mutations in genes encoding APC/C subunits genetically interact with *fzr*. Embryos carrying homozygous mutations for either *lmg* or *mr*, combined with one mutant copy of *fzr* reveal a strong myoblast fusion phenotype (E,E′,F,F′). In contrast, homozygous *lmg* and *mr* mutants alone do not show fusion arrest (A,A′,B,B′). Similarly, heterozygous *lmg* or *mr* mutants in combination with one mutant copy of *fzr* (C,C′,D,D′) do not display main myogenesis defects. However, single unfused myoblasts attached to nascent muscles can be observed (C′,D′). (G) Total myoblast number is increased in stage 13 and stage14 *fzr* mutants. While the overall number of myoblasts remains constant during fusion in wild type embryos, in *fzr* mutants it further increases after stage 13. (H) The number of rP298-lacZ-expressing cells, marking FCs and growing muscles, appears unaffected in *fzr* mutants before fusion starts at stage 13 and does not further increase until stage 14. (I) In *fzr*; *CycB* double mutants, myoblast numbers are restored to wild type levels. (J,K) The lack of *fzr* causes the appearance of phospho-histone 3 (PH3)-positive myoblasts (arrow in K), indicating additional cell divisions. (L,L′,M,M′,N,N′) Although myoblast numbers are restored, the fusion phenotype is not rescued in *fzr*;*CycB* double mutants. Boxed areas in A-F indicate magnified images A′-F′, respectively. Boxed areas in L-N indicate magnified images L′-N′, respectively. Double-headed arrows indicate muscle fibres, arrows indicate unfused myoblasts. Scale bars: 10 µm.

but were never observed in heterozygous *fzr*/+ animals. The reduction of *fzr* by one copy in either homozygous *lmg* or *mr* background caused complete failure of myoblast fusion (Fig. 4E,E′,F,F′). These data demonstrate a genetic interaction between *fzr* and genes that encode subunits of the APC/C during myoblast fusion, and we conclude that the observed muscle defects are due to a loss of APC/C function rather than an unknown, isolated function of *fzr*.

Given the role of the APC/C^{Fzr} in cell cycle control, we tested whether the number of myoblasts is altered in *fzr* mutant embryos.

Journal of Cell Science (2018) 131, jcs209155. doi:10.1242/jcs.209155

We counted all Mef2-positive myoblasts and found that wild type embryos exhibited ∼160 myoblasts per hemisegment at early stage 13, before the onset of fusion. This number remained constant until stage 14, indicating that myoblasts do not further divide and can be considered post-mitotic (Fig. 4G). By contrast, in *fzr* mutants the number of myoblasts at stage 13 was increased by ∼40% and increased even further until stage 14 (Fig. 4G and Table S1). Epithelial cells lacking *fzr* fail to exit the cell cycle and undergo one extra cell division, causing an approximately doubled cell number (Jacobs et al., 2002; Sigrist and Lehner, 1997). In *fzr* mutants, the number of myoblasts was not exactly doubled, suggesting that only part of the cells underwent extra divisions. The number of rP298-lacZ-expressing nuclei, marking FCs and growing myotubes, was not altered before fusion starts (early stage 13), indicating that FCs exit the cell cycle on time in *fzr* mutants (Fig. 4H). Compared to wild type animals, the number of rP298-lacZ-expressing cells in *fzr* mutants remained constant after stage 13 (Fig. 4H and Table S1). This can be explained by the lack of myoblast fusion and, thereby, a lack of recruitment of additional nuclei that express the reporter gene. Since the number of rP298-lacZ-positive nuclei was not affected before fusion and did not further increase later on, we concluded that the increase in the number of total myoblasts was mainly due to an increased number of FCMs. FCMs constitute a rather heterogeneous group of cells that undergo divisions after their specification in a non-synchronous manner. While the final FC division takes place during late stage 12, a small number of FCMs has been reported to divide until stage 13 (Beckett and Baylies, 2007).

Since the APC/C^{Fzr} reportedly controls the exit from the cell cycle, we tested whether the increased myoblast numbers were due to overproliferation, and whether this accounted for the observed fusion phenotype. Staining for phosphorylated histone 3, a reliable marker for mitotic cells (Gurley et al., 1978), revealed an increased number of mitotic cells in *fzr* mutant embryos (Fig. S1A,B). While most of these extra cell divisions took place in the epidermis of the embryo, co-staining with β3Tub also revealed myoblasts engaged in mitosis, and β3Tub was found to be highly enriched in the spindle of these dividing cells (Fig. 4J,K). One of the main ubiquitylation targets of APC/C during the cell cycle is CycB, and disruption of APC/C function leads to CycB accumulation and additional cell divisions (Sigrist and Lehner, 1997). In theory, mutations in CycB therefore counteract the cell cycle defects in *fzr* mutants since CycB should not accumulate. Indeed, *fzr;CycB* double mutants displayed myoblast numbers that were similar to wild type values, strongly suggesting that the cells regained their ability to exit their proliferative programme (Fig. 4I and Table S1). However, the same mutant embryos still displayed myoblast fusion defects (Fig. 4L-N′).

Therefore, we concluded that the APC/C^{Fzr} plays a dual role during myogenesis in the *Drosophila* embryo. On one hand, it seems to be essential to allow myoblasts to withdraw from the cell cycle. On the other hand, cell numbers alone are not sufficient to explain the observed fusion phenotype, indicating a second, most likely post-mitotic, role of the complex during cell-cell fusion.

APC/C^{Fzr} impacts on actin organisation

Since the recovery of myoblast number and, probably, the restoration of a timely controlled cell cycle exit in *fzr;CycB* double mutants did not result in a rescue of the fusion phenotype, we next investigated, whether the loss of *fzr* did impact on the fusion process directly. Myoblast fusion is essentially driven by the asymmetric nucleation of F-actin at the prospective fusion site between the FCM and the growing muscle. While FCMs accumulate a dense actin focus at the membrane, FCs form a thinner actin sheet along the fusion site (Kim et al., 2007; Schäfer et al., 2007; Sens et al., 2010). Importantly, while some of the proteins regulating the remodelling of the actin cytoskeleton are different, F-actin nucleation depends on the correct spatiotemporal activation of the Arp2/3-nucleation complex in both cell types. To test for impairment of actin nucleation, we visualised F-actin in wild type and mutant embryos at stage 13 and 14. We found that actin foci form in *fzr* mutants, indicating that the recruitment of the actin nucleation machinery to the prospective fusion site took place (red arrows in Fig. 5A-D″). We counted the average number of actin foci per hemisegment and found no significant differences between wild type and mutant embryos (Fig. 5E and Table S1). However, we did find a significant decrease in actin focus size in *fzr* mutants, suggesting impaired or incomplete actin nucleation at the fusion site (Fig. 5F and Table S1). Although our experimental setup did not allow us to quantitatively assess the amount of F-actin in a single FCM, our images nevertheless suggested that there was always increased enrichment of F-actin in FCMs compared to the FC, indicating that the asymmetric nature of actin nucleation was still intact (Fig. 5A′,B′,C′,D′). It has been shown previously that the high F-actin concentrations in the FCM cause a protrusive force, leading to invasion of the FC or myotube membrane (Sens et al., 2010). As a consequence of this mechanical stress, the FCs or growing myotubes increase membrane stiffness and/or rigidity as an opposing force to the actin focus. This is achieved by the accumulation of non-muscle myosin II (Myo II) at the fusion site, probably causing increased tensile forces along the membrane of the FC, which allows the two opposing membranes to come into closer contact with each other (Kim et al., 2015). Therefore, we visualised the appearance of Myo II clusters in areas where FCMs attached, to test whether the observed F-actin foci are able to generate an invasive force that is sufficient to induce a response in the FC. By exclusively expressing GFP.Myo II in FCs and growing myotubes of late stage 14 embryos, we found that – although actin foci are smaller in *fzr* mutants – GFP.Myo II still accumulated in areas where FCMs attached to the growing muscle (Fig. 5G-J″; dashed areas indicate attached FCMs).

These data suggest that APC/C^{Fzr} activity somehow affects the formation of actin foci. However, since we did observe MyoII accumulation in the area of the growing muscle where FCMs attached, it is questionable whether a reduced focus size is sufficient to explain the observed fusion defects in *fzr* mutants. Eventually, our observation prompted us to ask whether the observed actin foci and MyoII accumulations are actually sufficient to induce membrane breakdown, and whether fusion might be blocked afterwards.

The formation of fusion pores is inhibited in *fzr* mutants

Establishment of FC-FCM attachment, actin focus formation and MyoII accumulation are followed by the formation of fusion pores, and the subsequent breakdown of the membranes between two fusing myoblasts. To test whether fusion pores are formed in *fzr* mutants, we conducted a GFP diffusion assay (Gildor et al., 2009). In wild type embryos, cytoplasmic GFP was able to diffuse from a growing myotube into attached FCMs, indicating that the membranes between the cells are permeable enough to allow diffusion of the protein (red arrow in Fig. 6A). Although GFP diffusion was frequently observed in wild type embryos, all attached FCMs in amorphic or hypomorphic *fzr* mutants remained GFP negative (red arrows in Fig. 6B,C). This suggests, that no or very small fusion pores were formed in *fzr* mutants, and that this caused the fusion arrest.

Journal of Cell Science (2018) 131, jcs209155. doi:10.1242/jcs.209155

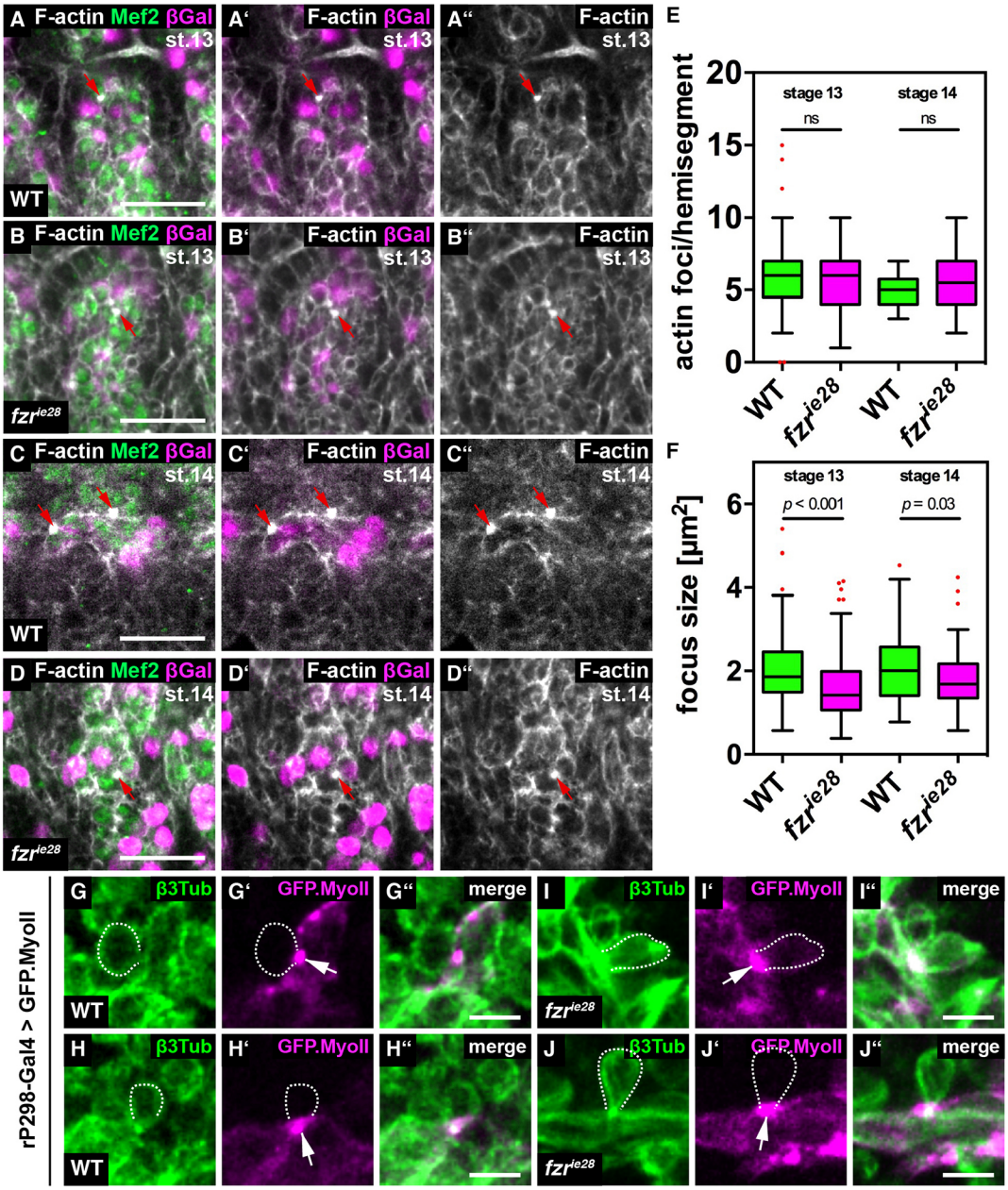

Fig. 5. F-actin foci number, foci size and MyoII localisation in wild type and *fzr* mutants at stage 13 and 14. (A-D″) F-actin foci (white), between FCs (magenta) and FCMs (green) in wild type (A,A′,A″ and C,C′,C″; WT) and *fzr* mutants (B,B′,B″ and D,D′,D″; fzr^{ie28}). Actin foci formed in mutant embryos. Images indicate the presence of a large actin focus in FCMs (red arrows). Scale bars: 10 µm. (E) Quantification of foci number per hemisegment. No significant differences were seen between *fzr* mutants and wild type. (F) Measurement of average focus size in *fzr* mutants and wild type. The average focus size was decreased in *fzr* mutants compared with WT. (G-J″) Accumulation of GFP-tagged Myosin II (MyoII, magenta) at the prospective fusion site. Two examples of FCMs attached to a nascent muscle in stage 15 wild type (G,H) and *fzr* mutant embryos (I,J) are shown. MyoII was exclusively expressed in the FC and growing muscle and accumulates in regions where FCMs attach to the muscle (arrows). Areas surrounded by dots indicate the outline of attached FCMs. Scale bars: 5 µm.

On the ultrastructural level, myoblast fusion can be divided into distinct morphological phases (Doberstein et al., 1997). By using transmission electron microscopy (TEM) analysis, a series of subcellular events were identified, including (1) the appearance of electron-dense vesicles at the fusion site (Fig. 6D), (2) the formation of electron-dense plaques along membranes (Fig. 6E) and (3) progressive membrane breakdown (Fig. 6F,G). Our initial assessment of fusion capability in the amorphic allele fzr^{ie28} revealed that fusion events are extremely rare (Figs 1I and 2E). However, we found that the hypomorphic allele fzr^{G0326} (Jacobs et al., 2002) shows an overall milder fusion phenotype, even though fusion was also arrested and no transfer of GFP was observed between myoblasts at stage 15 (Fig. S2 and Fig. 6B).

To maximize the chances of finding any myoblasts engaged in fusion in our ultrathin sections, we used the hypomorphic allele for our TEM analyses. Albeit all features of myoblast fusion were frequently found in wild type embryos (n=2 embryos), we rarely observed broken membranes in hypomorphic *fzr* mutants (n=4 embryos, Fig. 6H,I). This suggests that some myoblasts did form fusion pores at stage 13, which also explains the presence of multi-nucleated muscle precursors found in all *fzr* alleles tested (Fig. 2E). Altogether, the ultrastructural analysis of *fzr* mutant embryos

Journal of Cell Science (2018) 131, jcs209155. doi:10.1242/jcs.209155

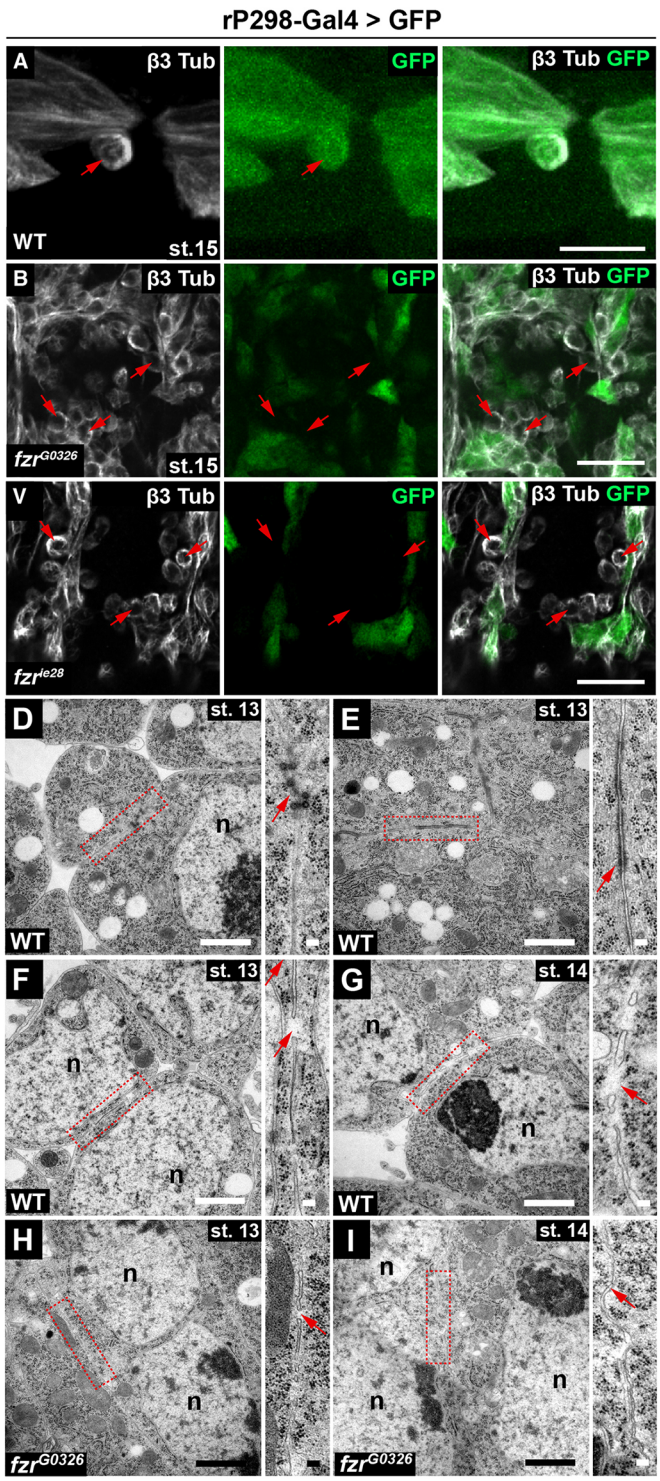

Fig. 6. Defective fusion pore formation in *fzr* mutant embryos. (A-C) FC-expressed cytoplasmic GFP is able to diffuse into attaching FCMs in wild type stage 15 embryos (red arrow in A). This was not observed in hypomorphic (*fzr*^{G0326}) or amorphic (*fzr*^{ie28}) mutants (B,C). Scale bars: 10 µm. (D-G) TEM sections of wild type embryos at stage 13 (D-F) reveal all fusion characteristics, including the appearance of electron-dense vesicles (D) and plaques (E) at the fusion site as well as fusion pore formation (F) (red arrows). (G) In stage 14 embryos, membrane breakdown can be frequently found between myoblasts (red arrow). (H,I) Rarely, fusion pores were visible in *fzr* mutants at stage 13 (red arrow in H), and never at stage 14, where most myoblast membranes remained intact (red arrow in I). Boxed areas in red within D-I are shown as magnified rectangular images to the right of each main image. Scale bars: 1 µm; 100 nm in magnified images.

indicate that a lack of fusion pore formation constitutes the most likely reason of the observed block in fusion.

Duf and Rols accumulate in *fzr* mutants

The remodelling of the actin cytoskeleton at the membranes between myoblasts requires the orchestrated activity of a well-described network of proteins (for review, see Schulman et al., 2015). The recognition and heterotypic adhesion between FCs and FCMs is mediated by a group of cell-type-specific Ig-domain-containing transmembrane proteins. While FCMs express Sticks and stones (Sns) and Hibris (Hbs), FCs express Dumbfounded (Duf, also known as Kirre) and Roughest (Rst) (Artero et al., 2001; Bour et al., 2000; Ruiz-Gómez et al., 2000; Strünkelnberg et al., 2001). In brief, upon binding through their extracellular domains, which also prevents homotypic adhesion between FCMs or FCs, the intracellular domains of Duf and Sns recruit specific adaptor proteins to the membrane, eventually resulting in the localised activation of the Arp2/3 actin-nucleation complex and formation of the observed actin foci (Kaipa et al., 2013; Richardson et al., 2007).

We tested a defined set of proteins involved in the transmission of the external signal towards the actin nucleation machinery – Sns, its downstream effector Blown fuse (Blow), Duf and Rolling pebbles [Rols, also known as Antisocial (Ants)], a direct binding partner of the intracellular domain of Duf (Fig. 7A-L). We monitored the overall localisation of each protein and measured signal intensities under controlled imaging conditions to estimate the relative abundance of those proteins in wild type and mutant embryos at late stage 12 or early stage 13, before the onset of fusion (for details see Materials and Methods, Table S1). In our hands, Sns localized to the entire cell membrane of FCMs, and neither its localisation nor relative abundance appeared changed in *fzr* mutants (Fig. 7A-C). Very similar results were obtained for Blow, which mainly localized to the cytoplasm of FCMs (Fig. 7D-F). This suggests that both proteins are expressed and localised normally in *fzr* mutants. In comparison, both Duf and Rols markedly accumulated in *fzr* mutant embryos (Fig. 7G-L). In wild type embryos, Duf was localised in distinct foci within the cell and at the membrane (Fig. 7G). However, in *fzr* mutants Duf accumulated at much higher concentrations and localized to large areas of the membrane and within the cytoplasm of the cell (Fig. 7H,I). This was also true for Rols, which displayed a higher abundance in *fzr* mutant animals and accumulated within the cytoplasm (Fig. 7J-L). As described above, Duf plays a role in mediating the initial recognition and attachment between myoblasts by binding with its own extracellular domain to the extracellular part of Sns on the side of the FCM (Ruiz-Gómez et al., 2000). However, its intracellular domain has been implicated in the activation of the actin nucleation machinery at the fusion site by recruiting Rols and other adaptor proteins to the membrane. (Bulchand et al., 2010; Chen and Olson, 2001; Haralalka et al., 2011). Finally, Rols has been suggested to play a second role in supporting the recycling of Duf back to the plasma membrane, allowing to reset the fusion machinery between two fusion events (Menon et al., 2005).

Thus, the observed accumulation of Duf and Rols in *fzr* mutants suggests direct involvement of the APC/C^{Fzr} in regulating the abundance of proteins involved in cell-cell fusion, leading to the question whether these proteins serve as direct targets of the complex.

Duf degradation depends on the proteasome, APC/C activity and three D-box motifs

From our results, we concluded that Duf and Rols might be direct substrates of the APC/C^{Fzr}. Target proteins are recognised by the

Journal of Cell Science (2018) 131, jcs209155. doi:10.1242/jcs.209155

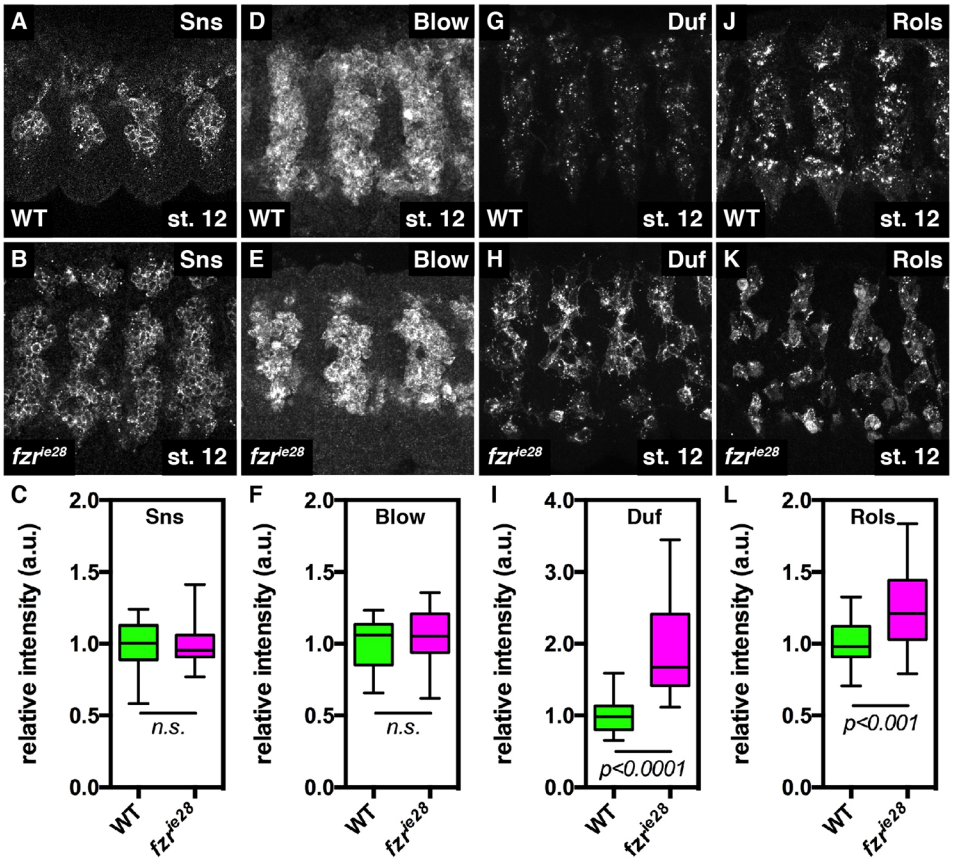

Fig. 7. Rols and Duf accumulate in *fzr* mutant myoblasts. (A,B,D,E,G,H,J,K) Stage 12/13 WT (A,D,G,J) and fzr^{ie28} mutant (B,E,H,K) embryos stained against Sns, Blow, Duf or Rols (three to four hemisegments). Localisation of Sns was the same in WT and *fzr* mutants (A,B). Similarly, the abundance and localisation of Blow was unaffected in *fzr* mutants (D,E). In wild type, Duf is localised in small clusters within the cytoplasm and at the membrane. However, lack of *fzr* causes Duf to be spread further along membranes and to accumulate within the cytoplasm (compare G with H). In a similar manner, Rols accumulates in the cytoplasm of *fzr* mutant myoblasts (compare J with K). (C,F,I,L) Relative fluorescence intensity [in arbitrary unit (a.u.)] of Sns, Blow, Duf and Rols. In WT compared with *fzr* mutant the fluorescence intensities of Blow and Sns are unchanged, whereas that of Rols and Duf show a significant increase.

APC/C^{Fzr} through two conserved degron motifs, the destruction box (D-box) and the Lys-Glu-Asn (KEN) box. To test whether Duf or Rols possess any of these motifs we used the GPS-ARM prediction algorithm (Liu et al., 2012).

Indeed, both proteins exhibit various potential D-boxes (Fig. 8A and data not shown). However, based on the immunostaining, it is unclear whether their accumulation was due to diminished protein degradation or whether it constituted a secondary effect caused by the absence of fusion itself. To test the impact of APC/C^{Fzr} activity on protein abundance, we expressed wild type Duf in S2 cells and treated the cultures with the proteasome inhibitor MG132 or the APC/C inhibitor TAME (Rock et al., 1994; Zeng et al., 2010). Duf accumulated in cells treated with either inhibitor, suggesting that both, the proteasome and the APC/C, are crucial regulators of Duf protein levels in cells (Fig. 8B). This indicated that Duf becomes degraded via the proteasome, and that the APC/C is involved in that degradation process. To test whether Duf is directly recognised by the APC/C, we expressed a version of Duf that lacks all potential D-box motifs (Duf^{mut}). The primary sequence of Duf contains three potential D-boxes, the presence of which is conserved in the human homologue KIRREL (Fig. 8A). Deletion of all three D-boxes caused a measurable accumulation of Duf^{mut} in S2 cells (Fig. 8C,D and Table S1), similar to what was observed in cells with inhibited proteasome- or APC/C-function. This strongly suggests that the D-Boxes in Duf are indeed functional and that the protein serves as a direct target of the APC/C.

Taken together these experiments provide first evidence that the APC/C^{Fzr} is crucial for myoblast fusion *in vivo*, by regulating the correct abundance and, probably, turnover of at least two proteins of the myoblast fusion machinery, and that at least one of them serves as direct target of the complex. Whether more proteins constitute targets of the complex or how this affects membrane fusion on the molecular level has yet to be investigated. Our findings extend the variety of post-mitotic functions of the APC/C^{Fzr}, and will certainly contribute a new perspective to the field of myoblast fusion.

DISCUSSION

In our present study, we identified the APC/C^{Fzr} as a novel regulator of muscle development. Our data suggest that the APC/C^{Fzr} functions during myogenesis, first, by defining the correct number of myoblasts before fusion, and second, by regulating the abundance of at least two proteins during the fusion process. This constitutes the very first *in vivo* description of a myogenic function of the APC/C^{Fzr}. However, more work will be needed to fully assess the various functions of this complex during muscle development.

A dual role for the APC/C^{Fzr} during muscle development

The mammalian Fzr homologue Cdh1, has been shown to fulfil a dual role during myogenesis in cultured myoblasts. On one hand, APC/C^{Cdh1} regulates ubiquitylation and, thereby, degradation of Skp2, an F-box protein and part of the ubiquitin ligase Skp1–Cul1–F-box protein (SCF) complex. Within SCF, Skp2 functions as a substrate-specific activator to allow the ubiquitylation and degradation of p27, a negative regulator of cell cycle progression. Consequently, lack of Cdh1 causes accumulation of Skp2, which results in a drop of p27 levels allowing myoblasts to continuously proliferate (Li et al., 2007). On the other hand, APC/C^{Cdh1} also targets the transcription factor Myf-5, a member of the MyoD family of myogenic regulatory factors (MRFs) (Zammit, 2017). In cultured myoblasts, this targeted degradation of Myf-5 has been suggested to be essential for myoblast differentiation and subsequent fusion (Li et al., 2007). Interestingly, *Drosophila* and other invertebrates only

Journal of Cell Science (2018) 131, jcs209155. doi:10.1242/jcs.209155

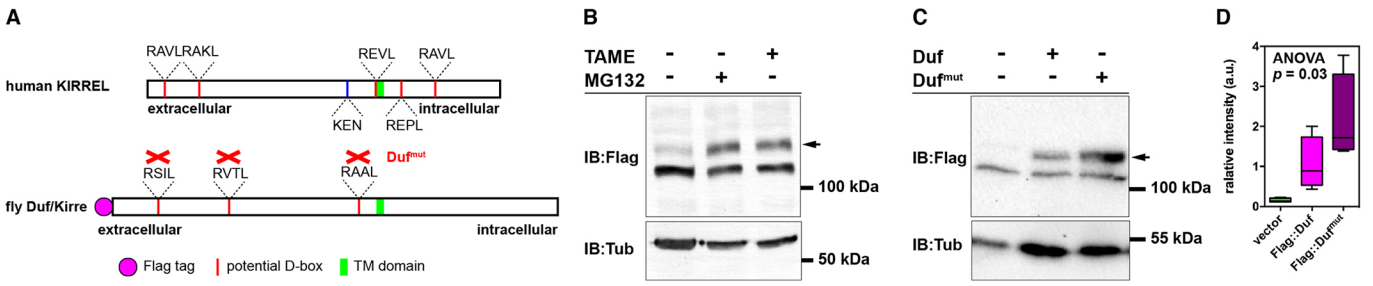

Fig. 8. Destruction of Duf depends on the proteasome and presence of three D-Box motifs. (A) Schematic representation of *Drosophila* Duf/Kirre (bottom) and its human homologue KIRREL (top). The location of potential D-Box motifs (consensus RxxL, in which x represents any aa) is highlighted in red. Red crosses indicate small deletions introduced into Duf/Kirre to abolish the potential D-Box motifs (Duf^{mut}). (B) Duf degradation depends on the proteasome and a functional APC/C. S2 cells expressing wild type Duf were either treated with vehicle control, the proteasome inhibitor MG132 or the inhibitor of the APC/C TAME. Treatment with either inhibitor caused an accumulation of Duf protein. (C) Compared to wild type Duf, Duf^{mut} accumulates in S2 cells, indicating that degradation of Duf depends on the presence of D-Box motifs. (D) Normalised densiometric measurements of Duf concentration from immunoblots. Compared to wild type Duf, Duf^{mut} shows an ∼2-fold increase within cultured S2 cells, further supporting the need of D-boxes for Duf degradation. Statistical differences between samples were calculated by one-way analysis of variance (ANOVA).

possess one homologous gene – Nautilus (Nau) – to the family of vertebrate MRFs (Michelson et al., 1990). However, during myogenesis Nau does not seem to play a general role in muscle differentiation but, rather, acts as an identity gene that is needed for the development of certain groups of muscles (Balagopalan et al., 2001). Overexpression of Nau, similarly, only affects certain muscle groups and has not been reported to block fusion (Keller et al., 1997).

Taken together we conclude that, like its vertebrate counterpart, *Drosophila* APC/C^{Fzr} plays a dual role in muscle development. We show that regulation of cell number and fusion capability are clearly independent of each other and, based on our experiments, we suggest that the increased number of myoblasts is due to overproliferation. At this point, it should be mentioned that an increase in cell numbers can also be achieved by other mechanisms, for example a lack of apoptosis. However, we present three lines of evidence, which – in our opinion – clearly show that extra cell divisions are the cause of the elevated myoblast numbers in *fzr* mutant embryos. First, we found increased levels of phosphorylated histone 3, a reliable marker for cells in mitosis. Second, *fzr,CycB* double mutants exhibited a reduction of myoblast numbers back to those of wild type (Table S1). And, last, the number of myoblasts increased in *fzr* mutants between stage 13 and 14, which cannot simply be explained by a lack of apoptosis (Fig. 4, Table S1). Taken together, we are confident that our data support the idea that the APC/C^{Fzr} is, indeed, regulating cell cycle withdrawal in *Drosophila* myoblasts.

The ubiquitin–proteasome pathway in *Drosophila* myogenesis

Although, no *in vivo* function of the APC/C during muscle development has been reported previously, our study is not the first description of involvement of the ubiquitin–proteasome pathway in *Drosophila* myogenesis. Mind bomb 2 (Mib2), another E3-ubiquitin ligase was shown to be expressed in FCs and to be involved in myoblast fusion, muscle attachment as well as sarcomere stability (Carrasco-Rando and Ruiz-Gómez, 2008; Domsch et al., 2017; Nguyen et al., 2007). Loss of *mib2* causes accumulation of the Gli-like transcription factor Lmd, which is expressed in all FCMs and crucial for the correct differentiation of these cells (Duan et al., 2001; Ruiz-Gómez et al., 2002). Furthermore, Lmd has been shown to be able to shuttle between the nucleus and cytoplasm of the cell (Duan and Nguyen, 2006). As a consequence, after FCMs have fused with nascent muscle fibres, Lmd needs to be removed from the cell to allow the correct differentiation programme, suggesting that Mib2 functions in maintaining the identity of the muscle during its development. Importantly, Mib2 has no influence on localisation or abundance of Duf and Rols, indicating that several ubiquitin ligases are active during myogenesis, which exhibit different substrate specificities and regulate different aspects of muscle development.

How does accumulation of Duf and Rols influence fusion?

In summary, our data strongly indicate that the most direct function of APC/C^{Fzr} during muscle development is the regulation of Rols and Duf levels in FCs and growing myotubes. However, the question remains: how does accumulation of either Rols or Duf cause a fusion arrest? Upon activation of Duf at the FC or myotube membrane, the intracellular part of the protein directly binds several proteins – including Rols, Schizo (also known as Loner) and the SH2/SH3 adaptor protein Dreadlock (Dock) – and recruits them to the membrane. Rols, in turn, recruits the guanidine nucleotide exchange factor (GEF) Myboblast city (Mbc), which further binds and activates the small GTPase Rac1. In parallel, Dock and Schizo recruit and activate the small GTPase Arf6, also resulting in Rac1 activation. Eventually, Rac1 functions to activate the nucleation-promoting factor SCAR/Wave, a direct regulator of the Arp2/3 actin nucleation machinery (Bulchand et al., 2010; Chen et al., 2003; Haralalka et al., 2011; Kaipa et al., 2013). In *fzr* mutants, the actin cytoskeleton seems to be only mildly affected, resulting in smaller actin foci between myoblasts (Fig. 5A-F). However, whether the smaller foci are causing the lack of fusion pores remains unclear. The observed smaller foci might be due to the mislocalisation of Duf and ectopic activation of the Arp2/3 complex outside the fusion site. This could, in turn, result in a competition for free G-actin and smaller foci. However, since we can detect MyoII accumulation in nascent *fzr* mutant muscles, the formed smaller foci seem to be sufficient to promote a mechanical force at the membrane. Nevertheless, the tension force produced might not be strong enough to induce membrane breakdown, causing an arrest of fusion and, maybe, preventing the formation of new fusion sites along the muscle. In addition, formation of F-actin foci is a very dynamic process and it is possible that, even if the basic machinery is able to nucleate actin in *fzr* mutants, the timely coordination of activation and deactivation is affected by higher levels of Duf and/or Rols. The number of actin foci remained constant between stage

13 and 14 in *fzr* mutants, although no fusion took place (Fig. 5E). This raises the questions why the size of the foci does not increase over time, and whether the foci formed at stage 13 become 'hyper-stable' and persist until later stages. Eventually, this needs to be tested in future experiments, addressing the dynamic behaviour of actin at the membrane.

In addition to its role in activating the Arp2/3 complex, Rols has also been suggested to function to dynamically recycle Duf back to the plasma membrane. Duf is present at the cell surface during the initial round of fusion but needs to be replenished at the membrane for subsequent fusion events in a Rols-dependent manner (Menon et al., 2005). Consequently, Rols null mutants exhibit multi-nucleated muscle precursors, whereas lack of Duf (in a double mutant with its partially redundant paralogue Rst) inhibits fusion completely, and all FCs remain mono-nucleated. This nicely fits our observation made in *fzr* mutants, in which even the strongest allele (*fzr*^{ie28}) does not abolish fusion completely (Fig. 2E). Together with our biochemical data (Fig. 8), this suggests that APC/C^{Fzr} is involved in the recycling of Duf after fusion and, thus, acts as a 'reset button' to prepare the muscle for the next round of fusion.

Taken together, we currently do not have enough data to completely elucidate the role of the APC/C^{Fzr} in muscle development. It will, therefore, be essential to investigate whether more substrates of the complex play a role during myogenesis, an option that has already been suggested because overexpression of Duf, Rols or both do not induce fusion defects (data not shown; see also Menon et al., 2005).

MATERIALS AND METHODS

Fly stocks and genetics

Fly strains: *fzr*^{H089}, *fzr*^{G129} and *fzr*^{GJ053} (C. Klämbt, University of Münster, Germany), *fzr*^{ie28} (C. Lehner, University of Zurich, Switzerland), *fzr*^{G0326}, *CycB*^{2}, *lmg*^{03424}, *mr*^{2}, Dp(1;3)DC120 (Bloomington Stock Center). rP298-lacZ,*fzr*^{ie28} and rP298-Gal4,*fzr*^{ie28} were generated by recombination. Strains for rescue and overexpression: rP298-lacZ;;UAS-Myc::Fzr and *fzr*^{ie28}/FM7c,*ftz*-lacZ;*mef2*-Gal4,UAS-mCD8::mRFP. GFP-tagged MyoII (Zipper) was expressed by crossing rP298-Gal4, *fzr*^{ie28} FM7c,*ftz*-lacZ females to FM7c,*ftz*-lacZ/Y;UAS-GFP.Zipper/+ males.

Gene specificity of the EMS alleles was proven genetically. Female *fzr*^{ie28}/FM7c,*B*^{1},*sn*^{1} flies were crossed to males carrying the genomic duplication Dp(1;3)DC120 to obtain *fzr*^{ie28}/Y;;Dp(1;3)DC120/+ males. This duplication is able to partially complement for the loss of *fzr* on the X chromosome but leaves a rough eye phenotype (data not shown). Subsequently, *fzr*^{EMS}/FM7c,*B*^{1},*sn*^{1} females were crossed to *fzr*^{ie28}/Y;; Dp(1;3)DC120/+ males and the progeny was screened for females that did not inherit the FM7c,*B*^{1},*sn*^{1} chromosome or the duplication and, hence, showed a normal eye pattern. If no such flies were obtained, the EMS chromosome was considered allelic to *fzr*^{ie28} and, therefore, gene specific. By using this assay, all identified EMS alleles of *fzr* proved to be allelic to *fzr*^{ie28}.

Immunofluorescence staining

Fly embryos were handled as described by Sellin et al. (2009). Primary antibodies used were guinea pig anti-β3 tubulin (1:5000, newly generated against a peptide described by Leiss et al., 1988), rabbit anti-Mef2 (1:500, H. Nguyen, University of Erlangen, Germany), rabbit anti-Lmd (1:500, H. Nguyen), rat anti-Kr (1:500, S. Roth, University of Cologne, Germany), mouse anti-Eve (1:5, cat. no. 2B8, DSHB), rabbit anti-Odd (1:200, J. Skeath, Washington University St. Louis, USA), rabbit anti-Tin (1:800, M. Frasch, University of Erlangen, Germany), rabbit anti-Svp [1:200 with TSA amplification kit (Perkin Elmer), J. Skeath], rabbit anti-Zfh1 (1:200, R. Lehmann, New York University, USA), rabbit anti-Blow (1:200, R. Renkawitz-Pohl, Philipps-University Marburg, Germany), rabbit anti-phosphorylated histone 3 (1:200, cat. no. 382159, Merck), mouse anti-GFP (1:500, cat. no. A11120, Thermo Fisher), mouse anti-Prc (1:5, cat. no. EC11, DSHB), rabbit anti-GFP (1:1000, cat. no. ab6556, Abcam), chicken anti-GFP (1:200, cat. no. ab13970, Abcam), mouse anti-β-galactosidase (1:200, cat. no. Z378A, Promega), rabbit anti-β-galactosidase (1:1000, cat. no. 55976, Cappel) and chicken anti-β-galactosidase (1:200, cat. no. ab9361, Abcam).

For rabbit anti-Rols (1:250, S. Önel, Philipps University Marburg, Germany), rabbit anti-Duf (1:500, K. F. Fischbach, Albert-Ludwigs-University Freiburg, Germany) and rabbit anti-Sns (1:200, K. F. Fischbach), embryos were heat-fixed as described by Albrecht et al. (2011). For F-actin staining, embryos were dechorionated in 50% bleach and fixed in 4% formaldehyde in 1× PBS for 25 min. The vitellin membrane was removed by incubating the embryos in a 1:1 mixture of heptane and 80% ethanol, and by rigorous shaking for 1 min. Embryos were allowed to settle for 5 min, the supernatant was then discarded and the procedure was repeated once. The embryos were quickly washed in ethanol three times, rehydrated by five 10 min washes in 1× PBS and immediately stained overnight at 4°C with TRITC-coupled phalloidin (Sigma-Aldrich). If double labelling was required, primary antibodies were added at this step. Secondary antibodies used were coupled to Cy2, Cy3 or Cy5 (1:200, Dianova), Alexa Fluor 543 or Alexa Fluor 633 (1:200, Life Technologies). Embryos were imaged on a Zeiss 5 Pascal upright cLSM and images were processed using Fiji (Schindelin et al., 2012).

Myoblast counting

Fly embryos where stained for Mef2 to label all myogenic cells, or βGal to label the rP298-lacZ reporter gene, as described above. Embryos were genotyped by using balancer chromosomes expressing either β-galactosidase or RFP. Image stacks, covering one embryonic hemisphere were acquired and myoblasts were manually counted in each hemisegment by using the Cell Counter plugin in Fiji.

Measurement of F-actin foci

Fly embryos were fixed and stained with TRITC-coupled phalloiodin and antibodies against Mef2 and β-galactosidase as stated above. *Z*-stacks of stage 13 and 14 embryos, covering one hemisphere, were acquired. Actin foci were manually counted in each hemisegment by using the Cell Counter plugin in Fiji. Actin foci size was determined by encircling each individual actin focus and measuring its area in μm^2 by using Fiji.

Intensity measurements

Fly embryos were fixed and stained as described above. Image acquisition was done under constant settings. Mean intensities were measured in ten 15×15 μm areas per embryo by using Fiji. Background values outside the musculature were measured in three areas of the same size. For each embryo, the ten intensity values were corrected against the background. To compare intensities across genotypes, the average of all background-corrected intensities from wild type or mutant animals was divided by the average of all background-corrected wild type intensities, resulting in normalised intensity values for all wild type and mutant animals (Fig. 7I-L).

TEM sections and imaging

Transmission electron microscopy (TEM) sections were carried out as published by Albrecht et al. (2011).

Generation of Duf D-box mutants

The Duf D-box deletion construct (Duf^{mut}) was generated with the Phusion Site-Directed Mutagenesis Kit (Thermo Fisher Scientific, Waltham, MA) using the coding sequence of wild type Flag::Duf (a gift from S. Önel) cloned into the pAc5.1/V5-His A vector, as a template.

Cell culture and immunoblotting

S2-cells were cultured as described by Wang et al. (2012). Cells were transfected using the Effectene (Qiagen) reagent, following the manufacturer's instructions. Cells were harvested 72 h after transfection and subjected to subsequent experiments. For inhibitor treatments, either 10 μM MG132 or 100 μM TAME was added to the cultures 48 h after transfection. Cells were harvested 12 h later.

Cells were homogenised in SDS-loading buffer and extracts were subjected to standard PA gel electrophoresis. Proteins were blotted on PVDF membrane. Antibodies used: rabbit anti-Flag (1:1000, cat. no. 4665.1, Carl Roth), mouse anti-βTub (E7, 1:100, DSHB), and HRP-coupled anti-rabbit and anti-mouse secondary antibodies (1:5000 and 1:10,000, respectively). Chemiluminescence was detected after 5 min incubation in freshly prepared Roti-Lumin (Carl Roth, Germany).

Statistics

Data were plotted as box-plots, whiskers indicating the min-to-max values. All values >1.5-fold interquartile distance were excluded and plotted as red dots. Sample sizes and statistical analysis can be found in Table S1.

Acknowledgements

We thank Kerstin Etzold, Mechthild Krabusch and Martina Biedermann for excellent technical assistance and TEM imaging. We also thank C. Klämbt, S. Önel, R. Renkawitz-Pohl, J. Skeath, K. F. Fischbach, R. Lehmann, M. Frasch, H. Nguyen, C. Lehner, S. Abmayr and A. Müller for sharing fly stocks, antibodies and reagents. We thank the Developmental Studies Hybridoma Bank (DSHB) for providing antibodies and the Bloomington Drosophila Stock Center (BDSC) for fly stocks.

Competing interests

The authors declare no competing or financial interests.

Author contributions

Conceptualization: M.D., A.P.; Methodology: M.D.; Investigation: M.D., H.M., A.C.W.; Writing - original draft: M.D., A.P.; Writing - review & editing: M.D., H.M., A.C.W., A.P.; Visualization: M.D.; Project administration: A.P.; Funding acquisition: M.D., A.P.

Funding

This work has been supported by grants from the French Muscular Dystrophy Association (AFM-Téléthon) to A.P. and M.D. (AFM FR_MYO), the Deutsche Forschungsgemeinschaft (DFG) to A.P. (SFB 944: Physiology and dynamics of cellular microcompartments), the Deutscher Akademischer Austauschdienst (DAAD) Procope-program, and the Niedersächsisches Ministerium für Wissenschaft und Kultur, Germany (grant no: ZN2832).

Supplementary information

Supplementary information available online at
http://jcs.biologists.org/lookup/doi/10.1242/jcs.209155.supplemental

References

Acquaviva, C. and Pines, J. (2006). The anaphase-promoting complex/cyclosome: APC/C. *J. Cell Sci.* **119**, 2401-2404.

Albrecht, S., Altenhein, B. and Paululat, A. (2011). The transmembrane receptor Uncoordinated5 (Unc5) is essential for heart lumen formation in *Drosophila melanogaster*. *Dev. Biol.* **350**, 89-100.

Artero, R. D., Castanon, I. and Baylies, M. K. (2001). The immunoglobulin-like protein Hibris functions as a dose-dependent regulator of myoblast fusion and is differentially controlled by Ras and Notch signaling. *Development* **128**, 4251-4264.

Azpiazu, N. and Frasch, M. (1993). *tinman* and *bagpipe*: two homeo box genes that determine cell fates in the dorsal mesoderm of *Drosophila*. *Genes Dev.* **7**, 1325-1340.

Balagopalan, L., Keller, C. A. and Abmayr, S. M. (2001). Loss-of-function mutations reveal that the *Drosophila nautilus* gene is not essential for embryonic myogenesis or viability. *Dev. Biol.* **231**, 374-382.

Bataillé, L., Delon, I., Da Ponte, J. P., Brown, N. H. and Jagla, K. (2010). Downstream of identity genes: muscle-type-specific regulation of the fusion process. *Dev. Cell* **19**, 317-328.

Bate, M. (1990). The embryonic development of larval muscles in *Drosophila*. *Development* **110**, 791-804.

Bate, M., Rushton, E. and Currie, D. A. (1991). Cells with persistent *twist* expression are the embryonic precursors of adult muscles in *Drosophila*. *Development* **113**, 79-89.

Beckett, K. and Baylies, M. K. (2007). 3D analysis of founder cell and fusion competent myoblast arrangements outlines a new model of myoblast fusion. *Dev. Biol.* **309**, 113-125.

Bodmer, R. (1993). The gene *tinman* is required for specification of the heart and visceral muscles in *Drosophila*. *Development* **118**, 719-729.

Bour, B. A., Chakravarti, M., West, J. M. and Abmayr, S. M. (2000). *Drosophila* SNS, a member of the immunoglobulin superfamily that is essential for myoblast fusion. *Genes Dev.* **14**, 1498-1511.

Braun, A., Meghini, F., Villa-Fombuena, G., Fernandez-Martinez, E., Glover, D., Martin-Bermudo, M. D., Gonzales-Reyes, A. and Kimata, Y. (2018). APC/C-Vihar regulates centrosome activity and stability in the *Drosophila* germline. doi: https://doi.org/10.1101/202465, *biorxiv.org*.

Bulchand, S., Menon, S. D., George, S. E. and Chia, W. (2010). The intracellular domain of Dumbfounded affects myoblast fusion efficiency and interacts with Rolling pebbles and Loner. *PLoS ONE* **5**, e9374.

Carrasco-Rando, M. and Ruiz-Gómez, M. (2008). Mind bomb 2, a founder myoblast-specific protein, regulates myoblast fusion and muscle stability. *Development* **135**, 849-857.

Chang, L. and Barford, D. (2014). Insights into the anaphase-promoting complex: a molecular machine that regulates mitosis. *Curr. Opin. Struct. Biol.* **29**, 1-9.

Chartier, A., Zaffran, S., Astier, M., Sémériva, M. and Gratecos, D. (2002). Pericardin, a Drosophila type IV collagen-like protein is involved in the morphogenesis and maintenance of the heart epithelium during dorsal ectoderm closure. *Development* **129**, 3241-3253.

Chen, E. H. and Olson, E. N. (2001). Antisocial, an intracellular adaptor protein, is required for myoblast fusion in Drosophila. *Dev. Cell* **1**, 705-715.

Chen, E. H., Pryce, B. A., Tzeng, J. A., Gonzalez, G. A. and Olson, E. N. (2003). Control of myoblast fusion by a guanine nucleotide exchange factor, loner, and its effector ARF6. *Cell* **114**, 751-762.

Das, D., Aradhya, R., Ashoka, D. and Inamdar, M. (2008). Macromolecular uptake in Drosophila pericardial cells requires rudhira function. *Exp. Cell Res.* **314**, 1804-1810.

Doberstein, S. K., Fetter, R. D., Mehta, A. Y. and Goodman, C. S. (1997). Genetic analysis of myoblast fusion: *blown fuse* is required for progression beyond the prefusion complex. *J. Cell Biol.* **136**, 1249-1261.

Dobi, K. C., Schulman, V. K. and Baylies, M. K. (2015). Specification of the somatic musculature in *Drosophila*. *Wiley Interdiscip Rev. Dev. Biol.* **4**, 357-375.

Domsch, K., Acs, A., Obermeier, C., Nguyen, H. T. and Reim, I. (2017). Identification of the essential protein domains for Mib2 function during the development of the *Drosophila* larval musculature and adult flight muscles. *PLoS ONE* **12**, e0173733.

Drechsler, M., Schmidt, A. C., Meyer, H. and Paululat, A. (2013). The conserved ADAMTS-like protein lonely heart mediates matrix formation and cardiac tissue integrity. *PLoS Genet.* **9**, e1003616.

Drysdale, R., Rushton, E. and Bate, M. (1993). Genes required for embryonic muscle development in *Drosophila melanogaster*-A survey of the X chromosome. *Rouxs Arch. Dev. Biol.* **202**, 276-295.

Duan, H. and Nguyen, H. T. (2006). Distinct posttranscriptional mechanisms regulate the activity of the Zn finger transcription factor lame duck during *Drosophila* myogenesis. *Mol. Cell. Biol.* **26**, 1414-1423.

Duan, H., Skeath, J. B. and Nguyen, H. T. (2001). *Drosophila* Lame duck, a novel member of the Gli superfamily, acts as a key regulator of myogenesis by controlling fusion-competent myoblast development. *Development* **128**, 4489-4500.

Figeac, N., Jagla, T., Aradhya, R., Da Ponte, J. P. and Jagla, K. (2010). *Drosophila* adult muscle precursors form a network of interconnected cells and are specified by the rhomboid-triggered EGF pathway. *Development* **137**, 1965-1973.

Follette, P. J. and O'Farrell, P. H. (1997). Cdks and the *Drosophila* cell cycle. *Curr. Opin. Genet. Dev.* **7**, 17-22.

Gajewski, K., Choi, C. Y., Kim, Y. and Schulz, R. A. (2000). Genetically distinct cardial cells within the *Drosophila* heart. *Genesis* **28**, 36-43.

Gildor, B., Massarwa, R., Shilo, B.-Z. and Schejter, E. D. (2009). The SCAR and WASp nucleation-promoting factors act sequentially to mediate *Drosophila* myoblast fusion. *EMBO Rep.* **10**, 1043-1050.

Gurley, L. R., D'Anna, J. A., Barham, S. S., Deaven, L. L. and Tobey, R. A. (1978). Histone phosphorylation and chromatin structure during mitosis in Chinese hamster cells. *Eur. J. Biochem.* **84**, 1-15.

Han, Z. and Bodmer, R. (2003). Myogenic cells fates are antagonized by Notch only in asymmetric lineages of the *Drosophila* heart, with or without cell division. *Development* **130**, 3039-3051.

Han, D., Kim, K., Kim, Y., Kang, Y., Lee, J. Y. and Kim, Y. (2009). Crystal structure of the N-terminal domain of anaphase-promoting complex subunit 7. *J. Biol. Chem.* **284**, 15137-15146.

Haralalka, S. and Abmayr, S. M. (2010). Myoblast fusion in *Drosophila*. *Exp. Cell Res.* **316**, 3007-3013.

Haralalka, S., Shelton, C., Cartwright, H. N., Katzfey, E., Janzen, E. and Abmayr, S. M. (2011). Asymmetric Mbc, active Rac1 and F-actin foci in the fusion-competent myoblasts during myoblast fusion in *Drosophila*. *Development* **138**, 1551-1562.

Hummel, T., Schimmelpfeng, K. and Klämbt, C. (1999). Commissure formation in the embryonic CNS of *Drosophila*. *Dev. Biol.* **209**, 381-398.

Ivy, J. R., Drechsler, M., Catterson, J. H., Bodmer, R., Ocorr, K., Paululat, A. and Hartley, P. S. (2015). Klf15 is critical for the development and differentiation of drosophila nephrocytes. *PLoS ONE* **10**, e0134620.

Jacobs, H. W., Richter, D. O., Venkatesh, T. R. and Lehner, C. F. (2002). Completion of mitosis requires neither *fzr*/*rap* nor *fzr2*, a male germline-specific *Drosophila* Cdh1 homolog. *Curr. Biol.* **12**, 1435-1441.

Kaipa, B. R., Shao, H., Schäfer, G., Trinkewitz, T., Groth, V., Liu, J., Beck, L., Bogdan, S., Abmayr, S. M. and Önel, S.-F. (2013). Dock mediates Scar- and

WASp-dependent actin polymerization through interaction with cell adhesion molecules in founder cells and fusion-competent myoblasts. *J. Cell Sci.* **126**, 360-372.

Keller, C. A., Erickson, M. R. S. and Abmayr, S. M. (1997). Misexpression of *nautilus* induces myogenesis in cardioblasts and alters the pattern of somatic muscle fibers. *Dev. Biol.* **181**, 197-212.

Kim, S., Shilagardi, K., Zhang, S., Hong, S. N., Sens, K. L., Bo, J., Gonzalez, G. A. and Chen, E. H. (2007). A critical function for the actin cytoskeleton in targeted exocytosis of prefusion vesicles during myoblast fusion. *Dev. Cell* **12**, 571-586.

Kim, J. H., Ren, Y., Ng, W. P., Li, S., Son, S., Kee, Y.-S., Zhang, S., Zhang, G., Fletcher, D. A., Robinson, D. N. et al. (2015). Mechanical tension drives cell membrane fusion. *Dev. Cell* **32**, 561-573.

Knirr, S., Breuer, S., Paululat, A. and Renkawitz-Pohl, R. (1997). Somatic mesoderm differentiation and the development of a subset of pericardial cells depend on the *not enough muscles (nem)* locus, which contains the *inscuteable* gene and the intron located gene, *skittles*. *Mech. Dev.* **67**, 69-81.

Kremser, T., Gajewski, K., Schulz, R. A. and Renkawitz-Pohl, R. (1999). Tinman regulates the transcription of the *beta3 tubulin* gene (*betaTub60D*) in the dorsal vessel of *Drosophila*. *Dev. Biol.* **216**, 327-339.

Lai, Z. C., Fortini, M. E. and Rubin, G. M. (1991). The embryonic expression patterns of *zfh-1* and *zfh-2*, two *Drosophila* genes encoding novel zinc-finger homeodomain proteins. *Mech. Dev.* **34**, 123-134.

Leiss, D., Gasch, A., Mertz, R. and Renkawitz-Pohl, R. (1988). β3 tubulin expression characterizes the differentiating mesodermal germ layer during *Drosophila* embryogenesis. *Development* **104**, 525-531.

Li, W., Wu, G. and Wan, Y. (2007). The dual effects of Cdh1/APC in myogenesis. *FASEB J.* **21**, 3606-3617.

Lilly, B., Galewsky, S., Firulli, A. B., Schulz, R. A. and Olson, E. N. (1994). D-MEF2: a MADS box transcription factor expressed in differentiating mesoderm and muscle cell lineages during *Drosophila* embryogenesis. *Proc. Natl. Acad. Sci. USA* **91**, 5662-5666.

Liu, Z., Yuan, F., Ren, J., Cao, J., Zhou, Y., Yang, Q. and Xue, Y. (2012). GPS-ARM: computational analysis of the APC/C recognition motif by predicting D-boxes and KEN-boxes. *PLoS ONE* **7**, e34370.

Lo, P. C. H. and Frasch, M. (2001). A role for the COUP-TF-related gene *seven-up* in the diversification of cardioblast identities in the dorsal vessel of *Drosophila*. *Mech. Dev.* **104**, 49-60.

Martins, T., Meghini, F., Florio, F. and Kimata, Y. (2017). The APC/C coordinates retinal differentiation with G1 arrest through the Nek2-dependent modulation of wingless signaling. *Dev. Cell* **40**, 67-80.

Meghini, F., Martins, T., Tait, X., Fujimitsu, K., Yamano, H., Glover, D.M. and Kimata, Y. (2017). Targeting of Fzr/Cdh1 for timely activation of the APC/C at the centrosome during mitotic exit. *Nat. Commun.* **7**, 12607.

Menon, S. D., Osman, Z., Chenchill, K. and Chia, W. (2005). A positive feedback loop between Dumbfounded and Rolling pebbles leads to myotube enlargement in *Drosophila*. *J. Cell Biol.* **169**, 909-920.

Michelson, A. M., Abmayr, S. M., Bate, M., Arias, A. M. and Maniatis, T. (1990). Expression of a MyoD family member prefigures muscle pattern in *Drosophila* embryos. *Genes Dev.* **4**, 2086-2097.

Nagy, O., Pál, M., Udvardy, A., Shirras, C. A., Boros, I., Shirras, A. D. and Deák, P. (2012). *lemmingA* encodes the Apc11 subunit of the APC/C in *Drosophila melanogaster* that forms a ternary complex with the E2-C type ubiquitin conjugating enzyme, Vihar and Morula/Apc2. *Cell Div.* **7**, 9.

Neuert, H., Yuva-Aydemir, Y., Silies, M. and Klämbt, C. (2017). Different modes of APC/C activation control growth and neuron-glia interaction in the developing Drosophila eye. *Development* **144**, 4673-4683. .

Nguyen, H. T., Voza, F., Ezzeddine, N. and Frasch, M. (2007). *Drosophila mind bomb2* is required for maintaining muscle integrity and survival. *J. Cell Biol.* **179**, 219-227.

Nose, A., Isshiki, T. and Takeichi, M. (1998). Regional specification of muscle progenitors in *Drosophila*: the role of the *msh* homeobox gene. *Development* **125**, 215-223.

Psathaki, O.-E., Dehnen, L., Hartley, P.S. and Paululat, A. (2018). Drosophila pericardial nephrocyte ultrastructure changes during ageing. *Mech. Ageing Dev.* **173**, 9-20.

Reed, B. H. and Orr-Weaver, T. L. (1997). The *Drosophila* gene *morula* inhibits mitotic functions in the endo cell cycle and the mitotic cell cycle. *Development* **124**, 3543-3553.

Richardson, B. E., Beckett, K., Nowak, S. J. and Baylies, M. K. (2007). SCAR/WAVE and Arp2/3 are crucial for cytoskeletal remodeling at the site of myoblast fusion. *Development* **134**, 4357-4367.

Rochlin, K., Yu, S., Roy, S. and Baylies, M. K. (2010). Myoblast fusion: when it takes more to make one. *Dev. Biol.* **341**, 66-83.

Rock, K. L., Gramm, C., Rothstein, L., Clark, K., Stein, R., Dick, L., Hwang, D. and Goldberg, A. L. (1994). Inhibitors of the proteasome block the degradation of most cell proteins and the generation of peptides presented on MHC class I molecules. *Cell* **78**, 761-771.

Rotstein, B., Post, Y., Reinhardt, M., Lammers, K., Buhr, A., Heinisch, J.J., Meyer, H. and Paululat, A. (2018). Distinct domains in the matricellular protein Lonely heart are crucial for cardiac extracellular matrix formation and heart function in Drosophila. *J. Biol. Chem.* **293**, 7864-7879.

Ruiz-Gómez, M., Romani, S., Hartmann, C., Jäckle, H. and Bate, M. (1997). Specific muscle identities are regulated by *Krüppel* during *Drosophila* embryogenesis. *Development* **124**, 3407-3414.

Ruiz-Gómez, M., Coutts, N., Price, A., Taylor, M. V. and Bate, M. (2000). *Drosophila* Dumbfounded: a myoblast attractant essential for fusion. *Cell* **102**, 189-198.

Ruiz-Gómez, M., Coutts, N., Suster, M. L., Landgraf, M. and Bate, M. (2002). *myoblasts incompetent* encodes a zinc finger transcription factor required to specify fusion-competent myoblasts in *Drosophila*. *Development* **129**, 133-141.

Schäfer, G., Weber, S., Holz, A., Bogdan, S., Schumacher, S., Müller, A., Renkawitz-Pohl, R. and Önel, S.-F. (2007). The Wiskott–Aldrich syndrome protein (WASP) is essential for myoblast fusion in *Drosophila*. *Dev. Biol.* **304**, 664-674.

Schindelin, J., Arganda-Carreras, I., Frise, E., Kaynig, V., Longair, M., Pietzsch, T., Preibisch, S., Rueden, C., Saalfeld, S., Schmid, B. et al. (2012). Fiji: an open-source platform for biological-image analysis. *Nat. Methods* **9**, 676-682.

Schulman, V. K., Dobi, K. C. and Baylies, M. K. (2015). Morphogenesis of the somatic musculature in *Drosophila melanogaster*. *Wiley Interdiscip Rev. Dev. Biol.* **4**, 313-334.

Sellin, J., Drechsler, M., Nguyen, H. T. and Paululat, A. (2009). Antagonistic function of Lmd and Zfh1 fine tunes cell fate decisions in the Twi and Tin positive mesoderm of *Drosophila melanogaster*. *Dev. Biol.* **326**, 444-455.

Sens, K. L., Zhang, S., Jin, P., Duan, R., Zhang, G., Luo, F., Parachini, L. and Chen, E. H. (2010). An invasive podosome-like structure promotes fusion pore formation during myoblast fusion. *J. Cell Biol.* **191**, 1013-1027.

Sigrist, S. J. and Lehner, C. F. (1997). *Drosophila fizzy-related* down-regulates mitotic cyclins and is required for cell proliferation arrest and entry into endocycles. *Cell* **90**, 671-681.

Silies, M. and Klämbt, C. (2010). APC/CFzr/Cdh1-dependent regulation of cell adhesion controls glial migration in the *Drosophila* PNS. *Nat. Neurosci.* **13**, 1357-1364.

Solomon, M. J. and Burton, J. L. (2008). Securin' M-phase entry. *Nat. Cell Biol.* **10**, 381-383.

Strünkelnberg, M., Bonengel, B., Moda, L. M., Hertenstein, A., de Couet, H. G., Ramos, R. G. and Fischbach, K. F. (2001). *rst* and its paralogue *kirre* act redundantly during embryonic muscle development in *Drosophila*. *Development* **128**, 4229-4239.

Su, M. T., Fujioka, M., Goto, T. and Bodmer, R. (1999). The *Drosophila* homeobox genes *zfh-1* and *even-skipped* are required for cardiac-specific differentiation of a numb-dependent lineage decision. *Development* **126**, 3241-3251.

van Roessel, P., Elliott, D. A., Robinson, I. M., Prokop, A. and Brand, A. H. (2004). Independent regulation of synaptic size and activity by the anaphase-promoting complex. *Cell* **119**, 707-718.

Volk, T., Wang, S., Rotstein, B. and Paululat, A. (2014). Matricellular proteins in development: perspectives from the *Drosophila* heart. *Matrix Biol.* **37**, 162-166.

Wang, S., Meyer, H., Ochoa-Espinosa, A., Buchwald, U., Önel, S.-F., Altenhein, B., Heinisch, J. J., Affolter, M. and Paululat, A. (2012). GBF1 (Gartenzwerg)-dependent secretion is required for *Drosophila* tubulogenesis. *J. Cell Sci.* **125**, 461-472.

Ward, E. J. and Skeath, J. B. (2000). Characterization of a novel subset of cardiac cells and their progenitors in the *Drosophila* embryo. *Development* **127**, 4959-4969.

Weber, U. and Mlodzik, M. (2017). APC/CFzr/Cdh1-dependent regulation of planar cell polarity establishment via Nek2 kinase acting on dishevelled. *Dev. Cell* **40**, 53-66.

Wilmes, A.C., Klinke, N., Rotstein, B., Meyer, H. and Paululat, A. (2018). Biosynthesis and assembly of the Collagen IV-like protein Pericardin in Drosophila melanogaster. *Biol. Open* **7**, bio030361.

Zammit, P. S. (2017). Function of the myogenic regulatory factors Myf5, MyoD, Myogenin and MRF4 in skeletal muscle, satellite cells and regenerative myogenesis. *Semin. Cell Dev. Biol.* **72**, 19-32.

Zeng, X., Sigoillot, F., Gaur, S., Choi, S., Pfaff, K. L., Oh, D.-C., Hathaway, N., Dimova, N., Cuny, G. D. and King, R. W. (2010). Pharmacologic inhibition of the anaphase-promoting complex induces a spindle checkpoint-dependent mitotic arrest in the absence of spindle damage. *Cancer Cell* **18**, 382-395.

Zielke, N., Querings, S., Rottig, C., Lehner, C. and Sprenger, F. (2008). The anaphase-promoting complex/cyclosome (APC/C) is required for rereplication control in endoreplication cycles. *Genes Dev.* **22**, 1690-1703.